[CANCER RESEARCH 62, 1978–1986, April 1, 2002]

Characterization of Benzo(*a*)pyrene-*trans*-7,8-dihydrodiol Glucuronidation by Human Tissue Microsomes and Overexpressed UDP-glucuronosyltransferase Enzymes[1]

Jia-Long Fang, Frederick A. Beland, Daniel R. Doerge, Doris Wiener, Chantal Guillemette, M. Matilde Marques, and Philip Lazarus[2]

Divisions of Cancer Control and Molecular Oncology, H. Lee Moffitt Cancer Center, Interdisciplinary Oncology Program and Departments of Biochemistry and Pharmacology and Therapeutics, University of South Florida, Tampa, Florida 33612 [J-L. F., D. W., P. L.]; Division of Biochemical Toxicology, National Center for Toxicological Research, Jefferson, Arkansas 72079 [F. A. B., D. R. D.]; Oncology and Molecular Endocrinology Research Center, CHUL Research Center (CHUQ), School of Pharmacy, Laval University, Quebec, Canada G1V-4G2 [C. G.]; and Centro de Química Estrutural, Complexo I, Instituto Superior Técnico, 1049-001 Lisboa, Portugal [M. M. M.]

ABSTRACT

UDP-glucuronosyltransferase (UGT)-mediated glucuronidation of benzo(*a*)pyrene-*trans*-7,8-dihydrodiol (BPD), precursor to the potent mutagen benzo(*a*)pyrene-7,8-dihydrodiol-9,10-epoxide, may be an important pathway in the detoxification of benzo(*a*)pyrene. To better characterize this pathway in humans, high-pressure liquid chromatography (HPLC) was used to detect glucuronide conjugates of BPD formed *in vitro*. Three peaks were detected by HPLC after incubation of racemic BPD with human liver microsomes; these were identified as monoglucuronides by liquid chromatography-mass spectrometry analysis. Proton nuclear magnetic resonance spectroscopy of isolated fractions, combined with HPLC analysis of the glucuronide products from human liver microsomal incubations with purified benzo(*a*)pyrene-*trans*-7*S*,8*S*-dihydrodiol [(+)-BPD] and benzo(*a*)pyrene-*trans*-7*R*,8*R*-dihydrodiol [(−)-BPD] forms of BPD, indicated that peak 1 contained the 7-glucuronide of 7*S*,8*S*-BPD (BPD-7S-Gluc), peak 2 was a mixture of the 7-glucuronide of 7*R*,8*R*-BPD (BPD-7R-Gluc) and the 8-glucuronide of 7*S*,8*S*-BPD (BPD-8S-Gluc), and peak 3 contained the 8-glucuronide of 7*R*, 8*R*-BPD (BPD-8*R*-Gluc). In liver microsomes, peak 1 (BPD-7S-Gluc) was the largest peak observed, whereas in microsomes from aerodigestive tract tissues, peak 2 (both BPD-7R-Gluc and BPD-8S-Gluc) was the largest HPLC peak observed. The liver enzymes UGT1A1 and UGT2B7 formed BPD-7S-Gluc as the major diastereomer, whereas UGT1A8 and UGT1A10, extrahepatic enzymes present in the aerodigestive tract, preferentially formed both BPD-7R-Gluc and BPD-8S-Gluc. In addition, both UGT1A9 and UGT1A7 preferentially formed BPD-7R-Gluc. No detectable glucuronidating activity against BPD was observed by UGT1A3, UGT1A4, UGT1A6, UGT2B4, UGT2B15, or UGT2B17. The affinity of individual UGT enzymes as determined by K_m analysis was UGT1A10 > UGT1A9 > UGT1A1 > UGT1A7 for (−)-BPD and UGT1A10 > UGT1A9 > UGT2B7 ~ UGT1A1 > UGT1A7 for (+)-BPD. These results suggest that several UGTs may play an important role in the overall glucuronidation of BPD in humans, with UGT1A1, UGT1A7, UGT1A9, UGT1A10 and potentially UGT1A8 playing an important role in the glucuronidation of the procarcinogenic (−)-BPD enantiomer, and that the stereospecific activity exhibited by different UGTs against BPD is consistent with tissue-specific patterns of BPD glucuronide diastereomer formation and UGT expression.

INTRODUCTION

BaP[3] is an extensively studied polycyclic aromatic hydrocarbon that is highly carcinogenic in animals, and its presence is widespread in the environment including in emission exhausts, cigarette smoke, and charbroiled foods (1–3). This carcinogen is metabolized by phase I enzymes to a large number of metabolites including phenols, arene oxides, quinones, dihydrodiols, and diol epoxides and is also conjugated by phase II enzymes to glutathione, sulfate, and UDPGA-derived glucuronic acid to form more water-soluble, detoxified derivatives (1). Although several of these metabolites contribute to the high carcinogenicity of BaP, numerous studies have clearly identified the 7,8-diol-9,10-epoxide as the primary carcinogenic metabolite of BaP, with the *anti*-(+)-BaP-7*R*,8*S*-dihydrodiol-9*S*,10*R*-epoxide diastereomer exhibiting enhanced mutagenic activity *in vitro* and *in vivo* (1, 2, 4–8). This penultimate carcinogen is formed from BaP by two rounds of cytochrome P450-mediated oxidation separated by a hydrolysis reaction involving epoxide hydrolase-mediated formation of the proximate carcinogen, BPD (see Fig. 1). In rats, 90–95% of BaP metabolism to the BaP-7,8-epoxide is to the (+)-[7*R*,8*S*] form (9, 10), and subsequent enzymatic hydrolysis of the (+)-[7*R*,8*S*]-epoxide results in formation of (−)-BPD. Upon oxidation, two isomeric diol-epoxides from each BPD enantiomer are formed, and although the relative amounts of each depend on the stereoselectivity of oxidation (8, 11, 12), conversion is primarily to the highly mutagenic *anti*-(+)-BaP-7*R*,8*S*-dihydrodiol-9*S*,10*R*-epoxide (9). Although less well-characterized than that in rats, the metabolic profiles reported from work with human tissues are similar to those reported for other mammalian systems (2).

The UGT superfamily of enzymes catalyzes the glucuronidation of a variety of compounds including endogenous compounds like bilirubin and steroid hormones, as well as xenobiotics including drugs and environmental carcinogens (13–16). Based on differences in sequence homology and substrate specificity, two families of UGTs (UGT1 and UGT2) have been identified in several species, each containing several highly homologous UGT genes. The entire UGT1 family is derived from a single locus on chromosome 2 that codes for nine functional proteins differing only in their NH_2 terminus because of alternate splicing of independent exon 1 regions to a shared COOH terminus encoded by exons 2–5 (17). In contrast to the UGT1A family, the UGT2B family is composed of several independent genes

Received 11/19/01; accepted 1/31/02.

The costs of publication of this article were defrayed in part by the payment of page charges. This article must therefore be hereby marked *advertisement* in accordance with 18 U.S.C. Section 1734 solely to indicate this fact.

[1] Supported by USPHS Grants R01-DE12206 and R01-DE13158 (National Institute for Dental and Craniofacial Research; to P. L.) and USPHS Grant P01–68384 (National Cancer Institute; P. L., project leader; Steven Stellman, principal investigator) from the NIH, Department of Health and Human Services.

[2] To whom requests for reprints should be addressed, at Divisions of Cancer Control and Molecular Oncology, H. Lee Moffitt Cancer Center, University of South Florida, MRC-2E, 12902 Magnolia Drive, Tampa, FL 33612. Phone: (813) 903-6820; Fax: (813) 632-1328; E-mail: plazarus@moffitt.usf.edu.

[3] The abbreviations used are: BaP, benzo(*a*)pyrene; BPD, benzo(*a*)pyrene-*trans*-7,8-dihydrodiol; UGT, UDP-glucuronosyltransferase; UDPGA, UDP glucuronic acid; HPLC, high-pressure liquid chromatography; NMR, nuclear magnetic resonance; (+)-BPD, benzo(*a*)pyrene-*trans*-7*S*,8*S*-dihydrodiol; (−)-BPD, benzo(*a*)pyrene-*trans*-7*R*,8*R*-dihydrodiol; BPD-7S-Gluc, benzo(*a*)pyrene-*trans*-7*S*,8*S*-dihydrodiol-7-glucuronide; BPD-8S-Gluc, benzo(*a*)pyrene-*trans*-7*S*,8*S*-dihydrodiol-8-glucuronide; BPD-7R-Gluc, benzo(*a*)pyrene-*trans*-7*R*,8*R*-dihydrodiol-7-glucuronide; BPD-8R-Gluc, benzo(*a*)pyrene-*trans*-7*R*,8*R*-dihydrodiol-8-glucuronide; LC, liquid chromatography MS, mass spectrometry; NOE, nuclear Overhauser effect; COSY, correlation spectroscopy; NOESY, nuclear Overhauser effect spectroscopy.

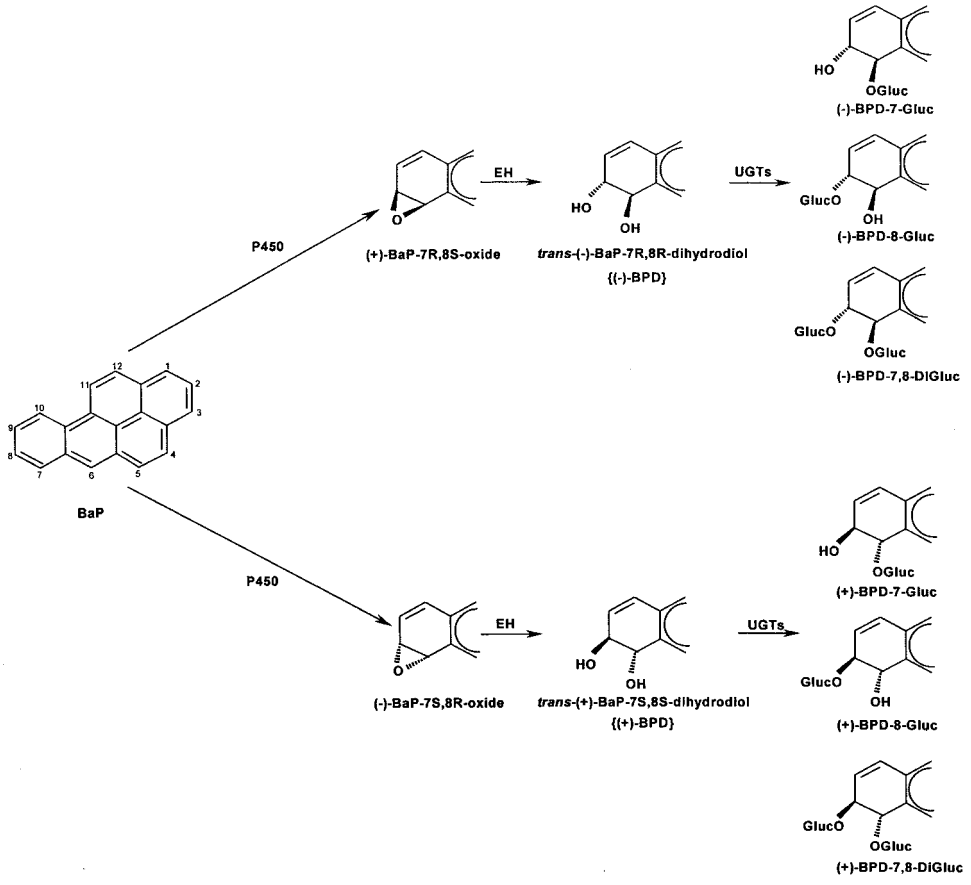

Fig. 1. Simplified schematic of BaP metabolism to BPD glucuronides and structures of potential BPD glucuronide regioisomers and diastereomers. *P450*, cytochrome P450; *EH*, epoxide hydrolase.

coding for seven known functional human UGT enzymes clustered on chromosome 4 (18–22).

Several studies have demonstrated that UGTs exhibit a protective effect against the carcinogenicity mediated by BaP. The addition of UDPGA to the Ames test is associated with a reduction in BaP mutagenicity (23, 24). In studies of UGT-deficient homozygous (j/j) and heterozygous (j/+) RHA rats *versus* UGT-normal (+/+) RHA controls, reduced glucuronidation of BaP metabolites *in vivo* was correlated with increased covalent binding to hepatic DNA and microsomal protein (25). In addition, a similar correlation was observed after *in vitro* incubations of BaP with rat liver microsomes, lymphocytes, or skin fibroblasts from UGT-deficient RHA rats (25–27). Although previous studies have shown that several UGTs, including UGT2B7, UGT1A7, UGT1A8, UGT1A9, and UGT1A10, exhibit glucuronidating activity against several phenolic derivatives of BaP (28–32), there is little information regarding the identity of the UGTs involved in the glucuronidation of BPD. In rats, to date, only UGT1A7 has been shown to exhibit activity against BPD (29, 33), whereas of the human UGTs yet tested, only UGT2B7 has been shown to possess activity (28). One of the potential reasons for the general failure to identify BPD-glucuronidating UGT enzymes in previous studies may lie with the fact that TLC was used as the method of detection in most previous studies. To obtain increased assay sensitivity and better characterize this pathway in humans, we have developed a HPLC assay to detect glucuronide conjugates of BPD. In the present study, we used this HPLC detection assay to identify the different BPD glucuronides formed in human liver and compare with the BPD glucuronides observed in potential target tissues of BaP exposure such as tissues of the aerodigestive tract. We demonstrate that several human UGTs exhibit stereo- and regiospecific glucuronidating activity against BPD and that the pattern of diastereomer/regioisomer formation observed for different UGTs is consistent with the patterns of BPD glucuronide diastereomer/regioisomer formation and differential UGT expression observed in different tissues. Implications regarding UGT enzyme involvement in BaP detoxification in potential target tissues are discussed.

MATERIALS AND METHODS

Chemicals and Materials. 3-Hydroxy-BaP, (+)-BPD, (−)-BPD, and racemic BPD were obtained from the National Cancer Institute Chemical Carcinogen Repository (synthesized and characterized at Midwest Research Institute, Kansas City, MO), dissolved in DMSO, and stored protected from light at −70°C. Imipramine, 1-naphthol, clofibric acid, androsterone, 4-nitrophenol, UDPGA, D,L-2-lysophosphatidyl choline palmital C16:0, and *Escherichia coli* β-glucuronidase were purchased from Sigma Chemical Co. (St. Louis, MO). [^{14}C]UDPGA was obtained from NEN Life Scientific Products (Boston, MA; specific activity = 380 Ci/mol). DMEM was obtained from Mediatech (Herndon, VA), and both fetal bovine serum and Geneticin (G418) were purchased from Life Technologies, Inc. (Grand Island, NY). Baculosome preparations overexpressing UGT1A1, UGT1A3, UGT1A7, UGT1A10, and UGT2B7 were purchased from PanVera Corp. (Madison, WI). HPLC-grade solvents were provided by various suppliers and used after filtration. All other chemicals were of analytical grade and used without further purification.

Tissue Samples and Microsome Preparation. Normal human liver tissues from patients undergoing hepatectomy were obtained from the Cooperative Human Tissue Network (Eastern Division, Philadelphia, PA). Normal human larynx and esophagus specimens were from individual patients undergoing cancer surgery at the H. Lee Moffitt Cancer Center and were obtained via the H. Lee Moffitt Cancer Center Tissue Procurement Facility. All protocols involving the analysis of tissue specimens were approved by the institutional review board at the University of South Florida and in accordance with assurances filed with and approved by the United States Department of Health and Human Services. Assurance was given by the Cooperative Human Tissue

Network that samples were isolated and quick-frozen at −70°C within 2 h after surgery.

Tissue microsomes were prepared through differential centrifugation as described previously (34) and stored (10–20 mg protein/ml) at −70°C in 100-μl aliquots, with total protein concentrations measured using the BCA assay (Pierce, Rockford, IL). Microsome preparations of UGT2B17-overexpressing cells were prepared as described previously (32).

Cell Lines and Cell Homogenate Preparation. HK293 (human embryonic kidney fibroblast) cells and HK293 cell lines overexpressing UGT1A4, UGT1A8, UGT2B1, UGT2B7, or UGT2B15 were kindly provided by Dr. Thomas Tephly (University of Iowa, Iowa City, IA; Refs. 35–40), whereas V79 (Chinese hamster fibroblast) cells and V79 cells overexpressing UGT1A6 and UGT1A9 were kindly provided by Dr. Brian Burchell (University of Dundee, Dundee, United Kingdom; Ref. 41). The stable transfectant of the UGT2B4-overexpressing cell line has been described previously (16).

All V79 and HK293 cell lines were grown to 80% confluence in DMEM supplemented with 4.5 mM glucose, 10 mM HEPES, 10% fetal bovine serum, 100 units/ml penicillin, and 100 μg/ml streptomycin and maintained in 700 μg/ml Geneticin for selection of UGT overexpression in a humidified incubator under an atmosphere of 5% CO_2. Cells were suspended in Tris-buffered saline [25 mM Tris base, 138 mM NaCl, and 2.7 mM KCl (pH 7.4)] and subjected to three rounds of freeze-thaw before gentle homogenization. Cell homogenates (5–30 mg homogenate protein/ml) were stored at −70°C in 100-μl aliquots. Total cell homogenate protein concentrations were determined using the BCA assay as described above.

Analysis of BPD Glucuronidating Activity. The rate of BPD glucuronidation was determined using the following conditions: tissue microsomes (1 mg of protein), cell homogenates (0.6–5 mg of protein), cell microsomes (50 μg of protein), or baculosomes (0.4–1.8 mg of protein) were incubated with 1–2 mM BPD, 4 mM UDPGA, and 1–2 μCi of [^{14}C]UDPGA (where indicated) in 10 mM $MgCl_2$ and 50 mM Tris-HCl (pH 7.4) in a total volume of 100–600 μl at 37°C for 2–16 h (as indicated in the text). Where indicated, incubations were performed with D,L-2-lysophosphatidyl choline palmital C16:0 (10 μg/100 μg protein) or in buffer containing 50 mM 3-(*N*-morpholino)propanesulfonic acid (pH 7.0) or 50 mM bis-Tris (pH 6.4). All reactions were initiated by the addition of UDPGA and terminated by the addition of an equal volume of ice-cold acetonitrile. Precipitates were removed by centrifugation (5 min, 14,000 × *g*), and supernatants were filtered and analyzed for glucuronidated BPD isomers by HPLC using a Beckman HPLC Gold System (Fullerton, CA) consisting of a model 110B programmable solvent module, a model 166 UV detector operated at 254 nm, a Waters automatic injector (model 717 plus), and a β-RAM radioisotope detector (IN/US, Tampa, FL) equipped with a 1 ml liquid flow cell. The samples were injected onto a 201TP (4.6 × 250 mm) 5 μ C_{18} 300 Å column (Vydac, Hesperia, CA). Separations were performed using the following linear gradient conditions: 0–5 min, 20% mixture A; 5–25 min, 20–40% mixture A; 25–30 min, 40–60% mixture A; 30–35 min, 60–90% mixture A, where mixture A was acetonitrile and was diluted at the given percentages in mixture B [20 mM NaH_2PO_4 (pH 4.6)]. The HPLC flow rate was 1 ml/min, whereas the scintillation fluid flow rate was 4 ml/min. The column was routinely washed with 100% mixture A for 15 min and equilibrated after every HPLC run with 20% mixture A for at least 20 min. Peaks corresponding to ^{14}C-glucuronide conjugates of BPD were tentatively identified by relative retention time and then confirmed by sensitivity to *E. coli* β-glucuronidase treatment (1000 units, overnight at 37°C) using HPLC as described above. For UGT-overexpressing cell homogenate or microsome experiments, the parent HK293 or V79 cell lines served as negative controls for all *in vitro* glucuronidation reactions. Kinetic analysis for all UGTs exhibiting significant glucuronidating activity against BPD was performed without detergent in Tris-Cl (pH 7.4) buffer as described above using 0.05–2 mM BPD and a maximal incubation time (0.5–4 h, as indicated) where the rate of BPD glucuronide formation was still linear for each UGT enzyme tested. The K_m and V_{max} for the glucuronidation of BPD by individual UGT enzymes were calculated after linear regression analysis of Lineweaver-Burk plots of at least three different experiments for each UGT enzyme examined. The detection limit for BPD glucuronide formation was about 5 pmol, with glucuronidation activities calculated based on radioflow detection and quantification of dpms within glucuronidated BPD-specific HPLC peaks as determined using the IN/US β_2 radioactivity detection program.

To confirm that all UGT-overexpressing cell homogenates, microsomes, and baculosomes tested in this study were active, glucuronidation assays were performed with known test substrates. HPLC was performed as described above for assays using 3-hydroxy-BaP as substrate for UGT1A1, UGT1A3, UGT1A7, UGT1A8, UGT1A9, UGT1A10, and UGT2B7. TLC analysis was performed as described previously (16, 42) for glucuronidation assays using 2 mM imipramine (UGT1A4), 1-naphthol (UGT1A6), clofibric acid (UGT2B4), 4-nitrophenol (UGT2B15), or androsterone (UGT2B17) as test substrate. As with BPD glucuronidation analysis, glucuronide formation for these test substrates was confirmed by treatment with *E. coli* β-glucuronidase as described above.

LC-MS Analysis of BPD Glucuronides. The LC separation of BPD glucuronides was performed using a Prodigy ODS-3 column (5 μ, 4.6 × 250 mm; Phenomenex Co., Torrance, CA) and a linear mobile phase gradient from 20% to 50% (v/v) acetonitrile in aqueous ammonium acetate [25 mM (pH 7)] over a 30-min period at a flow rate of 1.0 ml/min. The column effluent was split 1:5 before entry into the electrospray probe, with the remaining flow diverted to a UV detector to monitor absorption at 254 nm.

A Platform single quadrupole mass spectrometer (Micromass, Manchester, United Kingdom) equipped with an electrospray interface was used with an ion source temperature of 150°C. Positive and negative ions were acquired in full scan mode (*m/z* 100–800 using a 2-s cycle time). The mass spectrometer was calibrated over the mass range *m/z* 85–1200 using a solution of polyethylene glycols. Background-subtracted mass spectra were obtained by averaging spectra across the respective chromatographic peak and subtracting average background spectra immediately before and after this peak. At a sampling cone-skimmer potential of 30 V, the mass spectra consisted of predominantly the molecular species [*i.e.*, $(M + H)^+$ for the positive ion mode and $(M - H)^-$ for the negative ion mode]; increasing the voltage to 70 V produced diagnostic fragment ions from in-source collision-induced dissociation. LC-MS analysis was performed on samples from incubation mixtures containing unlabeled UDPGA.

NMR Analysis of BPD Glucuronides. ^{1}H NMR spectra were obtained on Bruker AM 500 MHz and Varian Unity INOVA 600 MHz spectrometers. Samples were dissolved in methanol-d_4. The chemical shifts (Table 1) are reported in ppm downfield from tetramethylsilane and the coupling constants (*J*) are reported in hertz. Assignments were made by comparison to the spectra of racemic BPD through the use of one-dimensional homonuclear decoupling experiments and observations of one-dimensional NOE enhancement patterns combined with two-dimensional COSY and 400-ms two-dimensional NOESY experiments.

RESULTS

Identification of BPD Glucuronide Regioisomers and Diastereomers in Human Liver Microsomes. As shown in Fig. 1, four BPD monoglucuronides and two BPD diglucuronides could potentially be formed via glucuronidation of BPD. Previous studies have not examined the possible formation of any of these glucuronides. To identify possible diastereomeric BPD derivatives formed in human liver, separation of BPD glucuronides was performed by HPLC using racemic BPD as substrate. A typical HPLC trace demonstrating BPD glucuronide formation after incubation of human liver microsomes with racemic BPD is shown in Fig. 2. Three peaks corresponding to predicted BPD glucuronides (retention time = 22–28 min) were detected by both UV detection (254 nm; Fig. 2*A*) and UDPGA-derived [^{14}C]glucuronic acid incorporation (Fig. 2*C*). These HPLC peaks were sensitive to treatment with β-glucuronidase (Fig. 2, *B* and *D*), confirming that they correspond to glucuronidated BPD conjugates.

It was originally hypothesized that the three HPLC peaks observed in our assays with human liver microsomes corresponded to the 7- and 8-monoglucuronides as well as the 7,8-diglucuronide of BPD. When the combined products of human liver microsomes were analyzed using LC with electrospray MS detection (Fig. 3), all three glucuronide peaks that had been observed by UV absorbance displayed molecular and fragment ions consistent with BPD monoglucuronide products. Each peak showed essentially the same negative ion mass

Table 1 *^{1}H NMR data for BPD 7- and 8-glucuronides*[a]

Proton	BPD	Peak 1	Peak 2	
		BDP-7S-Gluc	BDP-7R-Gluc	BPD-8S-Gluc
		*(ppm)		
1	8.20,[b] d[c]	8.19, m	8.19, m	8.19, m
2	8.00, t, $J_{1,2} = J_{2,3} = 7.6$	7.98, t, $J_{1,2} = J_{2,3} = 7.6$	7.99, m	7.99, m
3	8.18,[b] d	8.19, m	8.19, m	8.19, m
4	8.42, d	8.06, d, $J_{4,5} = 8.9$	8.10, m	8.10, m
5	8.42, d	8.19, m	8.10, m	8.10, m
6	8.09, s	8.79, s	8.76, s	8.48, s
7	5.08, d, $J_{7,8} = 10.8$	5.40, d, $J_{7,8} = 10.1$	5.35, d, $J_{7,8} = 10.8$	5.31, d, $J_{7,8} = 9.7$
8	4.58, ddd, $J_{7,8} = 10.1$; $J_{8,9} = 2.5$; $J_{8,10} = 2.1$	~4.87[d]	~4.8[d]	~4.8[d]
9	6.29, dd, $J_{9,10} = 10.1$; $J_{8,9} = 2.5$	6.27, dd, $J_{9,10} = 10.1$; $J_{8,9} = 2.3$	6.27, dd, $J_{9,10} = 10.1$; $J_{8,9} = 2.5$	6.58, dd, $J_{9,10} = 10.1$; $J_{8,9} = 2.2$
10	7.56, dd, $J_{9,10} = 10.1$; $J_{8,10} = 2.1$	7.55, dd, $J_{9,10} = 10.3$; $J_{8,10} = 2.3$	7.56, m	7.56, m
11	8.42, d, $J_{11,12} = 9.3$	8.41, d, $J_{10,11} = 9.4$	8.42, d, $J_{10,11} = 9.3$	8.43, d, $J_{10,11} = 9.4$
12	8.13, d	8.12, d, $J_{11,12} = 9.3$	8.10, m	8.10, m
1′		4.94, d, $J_{1',2'} = 7.3$	4.75, d, $J_{1',2'} = 7.3$	4.70, d, $J_{1',2'} = 7.7$

[a] Recorded in methanol-d_4.
[b] The assignment may be reversed.
[c] Abbreviations for coupling patterns: s, singlet; d, doublet; t, triplet; m, multiplet.
[d] Obscured by the residual methanol resonance; identified by two-dimensional COSY.

spectra, with deprotonated molecules [$(M - H)^-$] at = *m/z* 461. A prominent fragment ion corresponding to the phenol derived from elimination of the UDPGA moiety (*m/z* 267) was also observed, as were fragment ions from UDPGA (*m/z* 193, 175, and 113). Positive ion mass spectra consisted primarily of the phenol fragment ion (*m/z* 269), with smaller amounts of $(M + NH_4)^+$ at *m/z* 480 (data not shown).

The identity of the glucuronides was established by ^{1}H NMR analysis of the individual HPLC peaks, combined with information obtained from conducting incubations with the optically pure BDP isomers. To facilitate the interpretation, the spectrum of racemic BPD was obtained in the same solvent (methanol-d_4) that was used to analyze the glucuronide samples. The most noticeable feature in the BPD spectrum was the anticipated presence of two benzylic proton resonances, at 4.58 and 5.35 ppm, assigned to H8 and H7, respectively, on the basis of their coupling patterns (Table 1). Specifically, coupling to H7, H9, and H10 allowed the unequivocal assignment of H8, whereas H7 displayed only vicinal coupling to H8. As expected, all of the remaining protons of BPD were clearly in the aromatic region, with H4, H5, and H11 superimposed at 8.42 ppm (Table 1). H11 was distinguished from H12 on the basis of a NOE to H10, indicative of spatial proximity. H1 and H3, which are both coupled to H2, could not be assigned unequivocally. The structural analysis of the HPLC peaks containing individual glucuronides was mainly focused on changes in the BPD spectral pattern and on the characteristics of the H1′ proton of the UDPGA moiety due to its immediate vicinity to the BPD ring system. Because the remaining sugar protons provided little structural information, their chemical shifts are not listed in Table 1. Peak 1 (retention time = 23.5 min; Fig. 2*A*) contained a single component. As indicated in Table 1, the resonances of H1–H3 and H9–H12 were virtually unaffected by glucuronidation, which is consistent with their remoteness from the site of substitution. Whereas H4 and H5 where shifted upfield, presumably due to location in the shielding cone of the substituent, H6 underwent substantial deshielding (0.7 ppm), suggesting closeness to the substitution site. In addition, both H7 and H8 underwent a similar deshielding (~0.3 ppm) effect. As expected, two-dimensional COSY interactions (data not shown) were clearly present between H2 and H1/H3, H4 and H5, H7 and H8, H9 and H10, and H11 and H12. Likewise, two-dimensional NOESY cross-peaks (data not shown) existed between H1 and H2, H2 and H3, H4 and H5, H5 and H6, H9 and H10, H10 and H11, and H11 and H12. Although all these interactions were expected, they provided insufficient information for assigning the structure. The crucial structural evidence was afforded by the presence of a two-dimensional NOESY cross-peak between H7 and H1′, along with the concomitant absence of one between H1′ and H8, which indicated that the glucuronide contained in peak 1 was substituted at the 7 position of BPD.

Peak 2 (retention time = 25.5 min; Fig. 2*A*) contained two glucuronides (Table 1). The same two-dimensional COSY and two-dimensional NOESY interactions observed for peak 1 were present for the glucuronides in peak 2. One of the components had a NOE cross-peak between H1′ and H7, which indicated that it was a 7-substituted glucuronide. The second component in peak 2 had an upfield shift of H6 and a downfield shift of H9, compared with the other glucuronide in peak 2 and the glucuronide in peak 1, both of which are consistent with 8 substitution.

To examine the regio- and stereoselectivity of BPD glucuronide formation in human liver, microsomes were incubated with either (+)-BPD or (−)-BPD in individual reactions, and glucuronides were separated by HPLC. For assays using (+)-BPD as substrate (Fig. 2*E*), the ratio of HPLC peaks 1:2:3 was 29:1:0, whereas the ratio of HPLC peaks for assays using (−)-BPD (Fig. 2*F*) was 0:3.4:1. Combined with the results of ^{1}H NMR analysis indicating that peak 1 was comprised entirely of BPD glucuronidated at the 7 position, the fact that peak 1 was observed in incubations of human liver microsomes with (+)-BPD but not (−)-BPD indicated that peak 1 is BPD-7S-Gluc (see Fig. 1). Combined with ^{1}H NMR results demonstrating that peak 2 was comprised of BPD glucuronidated at both the 7 or 8 positions, the fact that peak 2 was observed in incubations with either (+)-BPD or (−)-BPD indicates that this peak is comprised of both BPD-8S-Gluc and BPD-7R-Gluc. Insufficient material was available to obtain NMR spectra on peak 3 (retention time = 26.3 min; Fig. 2*A*). Because the LC-MS data indicated that peak 3 was a monoglucuronide, and because peak 3 was formed only with (−)-BPD, we deduced that peak 3 contained BPD-8R-Gluc.

BPD Glucuronidation in UGT-overexpressing Cell Homogenates and Baculosomes. To elucidate whether any previously cloned human UGTs exhibit activity against BPD, we performed a comprehensive screening of known human UGTs for their activity against racemic BPD. All UGT-overexpressing cell homogenates and microsomes, as well as baculosome preparations from Sf-9 cells infected with UGT cDNA-containing baculovirus were active against known substrates for each of the UGTs examined in this study (results not shown). UGT1A8-, UGT1A9-, and UGT2B7-overexpressing cell lines as well as baculosomes overexpressing UGT1A1, UGT1A7, or UGT1A10 exhibited detectable levels of glucuronidating activity

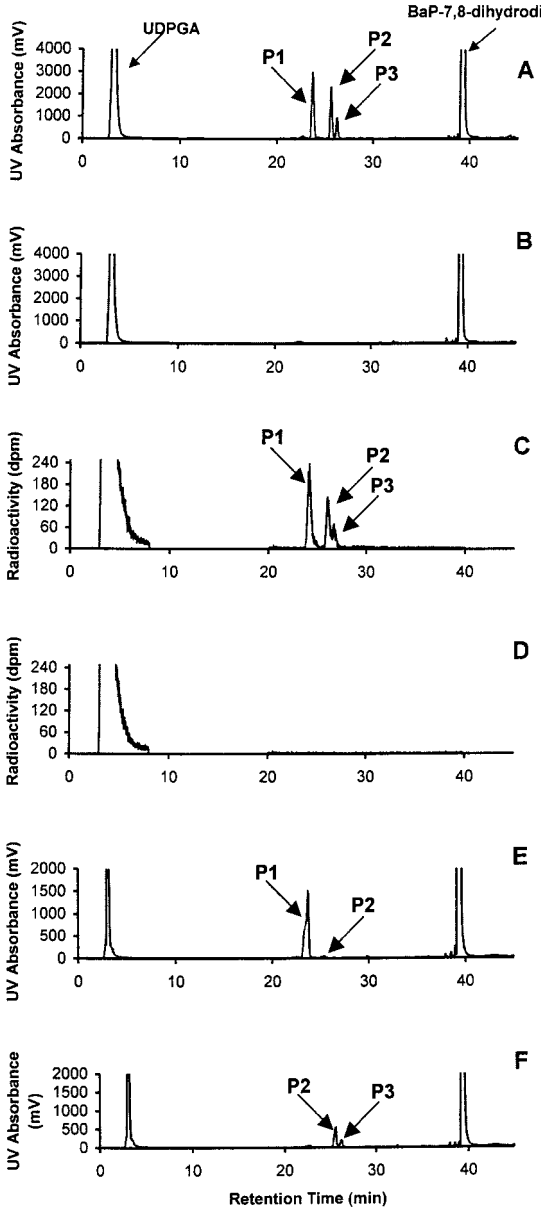

Fig. 2. HPLC analysis of BPD glucuronide formation by human liver microsomes. Human liver microsomes (1 mg of protein) were incubated at 37°C for 2 h with 1 mM BPD and 4 mM [^{14}C]UDPGA (1 μCi) as described in "Materials and Methods." *A–D*, incubations performed with racemic BPD; *E*, incubation performed with (+)-BPD; *F*, incubation performed with (−)-BPD. *A*, *B*, *E*, and *F*, BPD glucuronide formation as shown by UV detection (254 nm); *B*, BPD glucuronide formation as shown by UV detection (254 nm) in assays including β-glucuronidase as described in "Materials and Methods;" *C*, BPD ^{14}C-glucuronide formation as shown by radioactivity detection; *D*, BPD ^{14}C-glucuronide formation as shown by radioactivity detection in assays including β-glucuronidase as described in "Materials and Methods." BPD glucuronides corresponding to peaks 1 (*P1*), 2 (*P2*), and 3 (*P3*) are indicated by *arrows*.

against racemic BPD (Fig. 4). In all cases, the optimal rate of BPD glucuronide formation was observed in incubations without detergent (D,L-2-lysophosphatidyl choline palmital C16:0) and in Tris-HCl buffer (pH 7.4). No detectable glucuronidation of racemic BPD was observed for homogenates of cell lines overexpressing UGT1A4, UGT1A6, UGT2B4, or UGT2B15; for UGT1A3-overexpressing baculosomes; or for microsomes from UGT2B17-overexpressing cells in incubations, with or without detergent (D,L-2-lysophosphatidyl choline palmital C16:0) or in different buffer systems at various pHs (see "Materials and Methods"; results not shown).

As shown by HPLC, there were significant differences in the relative amount of BPD glucuronide diastereomers formed by homogenates from cells or baculosomes overexpressing the different UGTs in incubations with racemic BPD. The HPLC peaks 1:2:3 ratio exhibited by UGT1A1-overexpressing baculosomes was 1:0.5:0.2 (Fig. 4*A*), a ratio similar to that observed for human liver microsomes (1:0.4:0.1; see Fig. 2). In addition to being the major peak observed for homogenates of UGT1A1-overexpressing cells, HPLC peak 1, corresponding to the formation of BPD-7S-Gluc, was the only peak observed for incubations with homogenates from UGT2B7-overexpressing cells (Fig. 4*B*) or UGT2B7-overexpressing baculosomes (results not shown). UGT1A7 (Fig. 4*C*), UGT1A8 (Fig. 4*D*), UGT1A9 (Fig. 4*E*), and UGT1A10 (Fig. 4*F*) all exhibited a glucuronide diastereomer/regioisomer pattern with HPLC peak 2 (corresponding to the formation of BPD-7R-Gluc and/or BPD-8S-Gluc) being the major peak. Little or no peak 3 formation (corresponding to BPD-8R-Gluc) was observed for UGT1A1 (Fig. 4*A*)- or UGT1A7-overexpressing baculosomes (Fig. 4*C*) or for UGT1A9-overexpressing cell homogenates (Fig. 4*E*) in incubations with racemic BPD. Higher rates of HPLC peak 3 (BPD-8R-Gluc) *versus* peak 1 (BPD-7S-Gluc) formation were observed for homogenates from both UGT1A8 (Fig. 4*D*)- and UGT1A10 (Fig. 4*F*)-overexpressing cells.

To better characterize the stereo- and regiospecificity and the kinetics of each UGT against BPD enantiomers, reactions were performed using either (−)-BPD or (+)-BPD as the substrate. The BPD glucuronide isomer ratios observed by HPLC for the different UGTs and each BPD isomer [(+)-BPD and (−)-BPD; Table 2] were consistent with the HPLC peak ratios observed for racemic BPD (Fig. 4). For UGT1A1- and UGT1A7-overexpressing baculosomes and UGT1A9-overexpressing cell homogenates, HPLC peak 1 was preferentially formed in incubations with (+)-BPD, whereas HPLC peak 2 was preferentially formed in incubations with (−)-BPD, indicating that these UGTs preferentially glucuronidate the 7 position of BPD. HPLC peak 2 was the major peak for both UGT1A7- and UGT1A9-overexpressing cell homogenates, whereas peak 1 was the major peak for UGT1A1-overexpressing cell homogenates in incubations with racemic BPD. These data suggest that UGT1A1 preferentially forms BPD-7S-Gluc, whereas UGT1A7 and UGT1A9 preferentially form BPD-7R-Gluc. Consistent with observations in incubations with racemic BPD, homogenates from UGT2B7-overexpressing cells exhibited significant activity against (+)-BPD, with HPLC peak 1 (corresponding to BPD-7S-Gluc) being the only peak observed; no detectable activity was observed for UGT2B7-overexpressing cell homogenates against (−)-BPD. HPLC peaks 2 and 3 were both observed for incubations of UGT1A8- and UGT1A10-overexpressing baculosomes with (−)-BPD, whereas HPLC peak 2 was preferentially formed in incubations with (+)-BPD, indicating that both the 7 and 8 positions of (−)-BPD and the 8 position of (+)-BPD were glucuronidated by these UGTs.

The relative affinities for each BPD enantiomer as reflected by the apparent K_m were UGT1A10 > UGT1A9 > UGT2B7 ~ UGT1A1 ≫ UGT1A7 for (+)-BPD and UGT1A10 > UGT1A9 > UGT1A1 > UGT1A7 for (−)-BPD (Table 2). UGT1A10 and UGT1A9 exhibited similar affinity for both the (−)-BPD and (+)-BPD, whereas UGT1A7 and UGT1A1 exhibited higher affinity for (−)-BPD. Consistent with the isomer patterns observed in incubations with either racemic BPD or each of the purified (+)-BPD or (−)-BPD enantiomers, UGT2B7 exhibited higher overall activity for (+)-BPD as compared with (−)-BPD (as determined by the V_{max}:K_m ratio), whereas UGT1A7 and UGT1A9 exhibited higher overall activity for (−)-BPD. Similarly, the high levels of HPLC peak 2 formation observed for both UGT1A1 and UGT1A10 with racemic BPD (Fig. 4) are consistent with their similar overall activity for each of the purified BPD enantiomers (Table 2). Although UGT1A8 exhibited

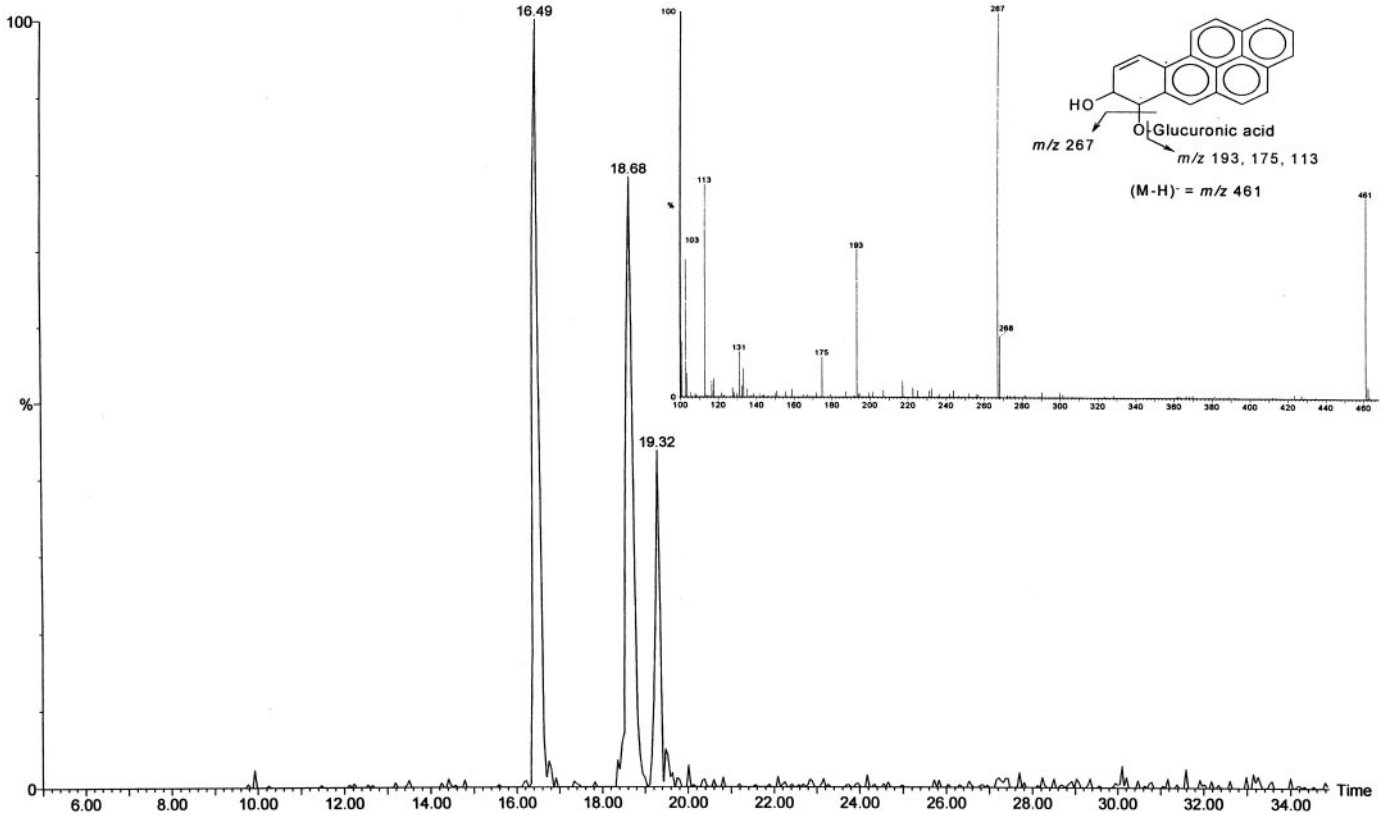

Fig. 3. LC-MS analysis of BPD glucuronides formed from incubations with human liver microsomes. BPD was incubated with human liver microsomes as described in "Materials and Methods," and the combined products were analyzed using LC with electrospray MS in the negative ion detection mode. The trace shown (*m/z* 461) is from the deprotonated molecule $(M - H)^-$ for isomeric BPD monoglucuronides. The *inset* mass spectrum, representative of all BPD monoglucuronides, was acquired using a sampling cone skimmer potential of 70 V to produce diagnostic fragment ions.

detectable levels of activity against racemic BPD (see Fig. 4*D*), kinetic analysis could not be performed due to low overall rates of BPD glucuronide formation for the UGT1A8-overexpressing cell line.

BPD Glucuronidation in Aerodigestive Tract Tissues. Previous studies have demonstrated differential expression of UGTs in different human tissues (31, 43–46). To better assess the role of differential UGT expression on BPD glucuronidation in aerodigestive tract tissues (target tissues for BaP exposure), separation of BPD glucuronides by HPLC was performed for both human laryngeal (Fig. 5*A*) and esophageal (Fig. 5*C*) microsomes after incubation with racemic BPD. As observed for human liver microsomes, three peaks corresponding to predicted BPD glucuronides (retention time = 22–28 min) were detected. These HPLC peaks were sensitive to treatment with β-glucuronidase (Fig. 5, *B* and *D*). The levels of total BPD glucuronide formation in liver microsomes were approximately 250- and 500-fold that observed for laryngeal and esophageal microsomes, respectively, in incubations with racemic BPD. In contrast to human liver microsomes, in which HPLC peak 1 was the preferential peak formed (comprising 71% of the total BPD glucuronide peaks), peak 2 was the preferential peak formed with microsomes from both aerodigestive tract tissues, with peak 1 comprising only 36% and 10% of the total BPD glucuronide peaks for laryngeal and esophageal microsomes, respectively (see Fig. 1). The pattern of stereo- and regiospecificity in aerodigestive tract tissues is similar to that observed for the aerodigestive tract tissue expressing UGT1A7, UGT1A8, and UGT1A10.

DISCUSSION

This is the first study to characterize the glucuronidation of BPD by human UGTs. Several human UGTs were shown to exhibit significant levels of activity against BPD, with different UGT enzymes exhibiting specific patterns of stereo- and regioselective BPD-monoglucuronide diastereomer/regioisomer formation. Whereas the UGT with the lowest K_m and therefore the highest affinity for both (+)-BPD and (−)-BPD was UGT1A10, other UGTs including UGT1A1, UGT1A7, UGT1A8, and UGT1A9 also exhibited detectable levels of activity against both BPD enantiomers, whereas UGT2B7 exhibited significant levels of activity against (+)-BPD. Of these, only UGT2B7 has been shown to exhibit activity against BPD in previous studies (28). No activity against BPD was observed for UGT1A8 and UGT1A10 in transiently transfected COS-7 cells (30), whereas no detectable glucuronidation of BPD was observed for HK293 cells stably transfected with human UGT1A7 (32). It is likely that these discrepancies are due to decreased assay sensitivity in previous studies. In contrast to the transient transfection studies of Mojarrabi and Mackenzie (30), the UGTs analyzed in the present study were from either stably transfected cell lines or overexpressing baculosomes. Moreover, whereas a sensitive HPLC assay was used to detect BPD-glucuronide formation in the present study, TLC was used to detect BPD-glucuronidating activities in previous studies (28, 30, 32).

In addition to increased sensitivity, the HPLC methodology used in the present study allowed for the detection and identification of individual BPD glucuronide isomers. As shown by mass and ^{1}H NMR spectral analyses, none of the BPD glucuronides detected by HPLC in this study were diglucuronides; all were monoglucuronides at either the 7 or 8 position of BPD. Of the four possible BPD monoglucuronide isomers formed by glucuronidation of BPD, both the 7*S*- and 8*R*-glucuronides (HPLC peaks 1 and 3, respectively) were separated from other potential BPD glucuronide isomers using the HPLC meth-

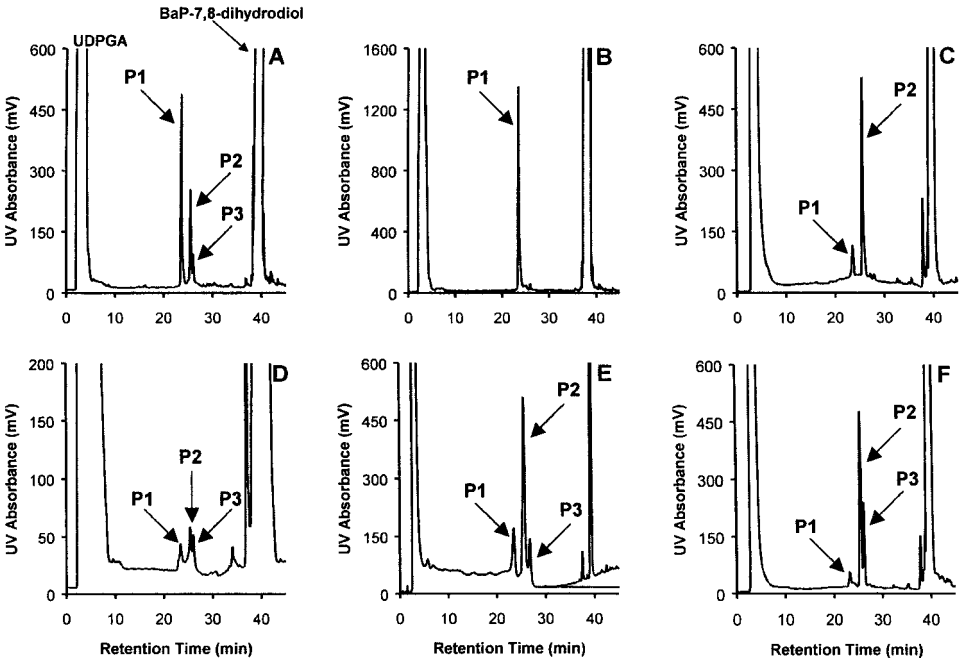

Fig. 4. HPLC analysis of BPD glucuronide formation in homogenates from UGT-overexpressing V79 and HK293 cells and UGT-overexpressing baculosomes. Cell homogenates or baculosomes were incubated at 37°C with 1 mM racemic BPD and 4 mM UDPGA as described in "Materials and Methods." Shown are metabolites from incubations using UGT1A1-overexpressing baculosomes (0.8 mg of protein) (*A*), homogenates (0.6 mg of protein) from UGT2B7-overexpressing HK293 cells (*B*), UGT1A7-overexpressing baculosomes (1.8 mg of protein; *C*), homogenates (5 mg of protein) from UGT1A8-overexpressing HK293 cells (*D*), homogenates (1 mg of protein) from UGT1A9-overexpressing V79 cells (*E*), and UGT1A10-overexpressing baculosomes (0.4 mg of protein; *F*). Assays were performed for 2 h for incubations with UGT1A1, UGT2B7, UGT1A7, UGT1A9, and UGT1A10 and for 16 h for incubations with UGT1A8.

odology described in this study. Unfortunately, the 7*R*- and 8*S*-glucuronides (comprising HPLC peak 2) could not be separated despite the use of several different separation columns and elution procedures (results not shown).

Of the UGTs shown in previous studies to be expressed in human liver, UGT1A1, UGT1A9, and UGT2B7 exhibited detectable levels of activity against BPD isomers in this study, with glucuronidation preferentially at the 7-hydroxy position of BPD for all three UGTs. As shown in incubations with either racemic BPD or the purified BPD forms [(+)-BPD *versus* (−)-BPD] and confirmed by kinetic analysis, UGT1A1 preferentially formed BPD-7S-Gluc, a pattern similar to that observed for human liver microsomes. UGT2B7 formed exclusively BPD-7S-Gluc, whereas BPD-7R-Gluc was preferentially formed by UGT1A9. These results suggest that all three of these UGTs could play an important role in the glucuronidation of BPD in human liver.

All three of the known extrahepatic UGTs (UGT1A7, UGT1A8, and UGT1A10) exhibited activity against BPD in our studies. Of these, UGT1A10 appeared to have the highest affinity for (+)-BPD and (−)-BPD, although the K_m of UGT1A8 for BPD could not be tested in our studies. In contrast to what was observed for human liver microsomes, which form predominantly BPD-7S-Gluc in incubations with racemic BPD, the major glucuronides formed for UGT1A8 and UGT1A10 are BPD-7R-Gluc, BPD-8R-Gluc, and BPD-8S-Gluc, whereas BPD-7R-Gluc is preferentially formed by UGT1A7. This pattern of stereo- and regioselectivity is consistent with the fact that these enzymes are not expressed in the liver and is similar to that observed with microsomes prepared from tissues of the human aerodigestive tract. Both human esophageal and laryngeal microsomes exhibit an HPLC peak pattern similar to that observed for these extrahepatic UGTs, with HPLC peak 2 being the major form observed in incubations with racemic BPD. This is consistent with the fact that UGT1A7 and UGT1A10 are well expressed in all aerodigestive tract tissues examined thus far and with the fact that UGT1A8 is expressed in the larynx (46). Although the total BPD glucuronidation observed for liver microsomes is significantly greater than that observed for aerodigestive tract tissues in incubations with racemic BPD, this difference is dramatically decreased when BPD-7S-Gluc [peak 1, formed by glucuronidation of (+)-BPD] is excluded from this comparison. Together, these data suggest that one or more of these extrahepatic UGTs may play an important role in the detoxification of (−)-BPD in aerodigestive tract tissues.

Because the highly mutagenic *anti*-(+)-BaP-7*R*,8*S*-dihydrodiol-9*S*,10*R*-epoxide is formed by oxidation of (−)-BPD (9), glucuronidation of this BPD enantiomer may be an important mechanism by

Table 2 *Kinetic analysis of the glucuronidation of BPD isomers by human UGT enzymes*

	(−)-BPD				(+)-BPD			
	K_m (μM)	V_{max} (pmol min^{-1} mg^{-1})	V_{max}/K_m (μl min^{-1} g^{-1})	BPD-7R-Gluc: BPD-8R-Gluc[a]	K_m (μM)	V_{max} (pmol min^{-1} mg^{-1})	V_{max}/K_m (μl min^{-1} g^{-1})	BPD-7S-Gluc: BPD-8S-Gluc[b]
UGT1A1[c]	290 ± 17[d]	5.0 ± 0.5	17	1:0.3	392 ± 47	13 ± 1.4	32	1:0.1
UGT1A7	695 ± 62	0.8 ± 0.2	1.2	1:0	1442 ± 308	0.3 ± 0.07	0.2	1:0
UGT1A8		Not performed[e]		1:1.2		Not performed[e]		0:1[a]
UGT1A9	244 ± 22	166 ± 17	680	1:0.4	241 ± 29	36 ± 4.4	149	1:0.2
UGT1A10	183 ± 20	9.3 ± 0.4	51	1:1.0	189 ± 21	16 ± 2.6	84	1:6.6
UGT2B7	ND[f]	ND	ND		361 ± 3.8	36 ± 0.6	100	1:0

[a] BPD glucuronide regioisomer ratios were calculated based on HPLC peak areas, with peak 2 as the referent.
[b] BPD glucuronide regioisomer ratios were calculated based on HPLC peak areas, with peak 1 as the referent.
[c] Incubations were performed without detergent in Tris-Cl (pH 7.4) buffer at 37°C for 2 (UGT1A1, UGT1A9, and UGT1A10), 4 (UGT1A7), 16 (UGT1A8), or 0.5 h (UGT2B7), as indicated in "Materials and Methods."
[d] Data are presented as mean ± SD for three independent experiments.
[e] Kinetic analysis was not performed for UGT1A8 due to low overall glucuronidating activity of UGT1A8-overexpressing cell homogenates (see text).
[f] ND, not detectable.

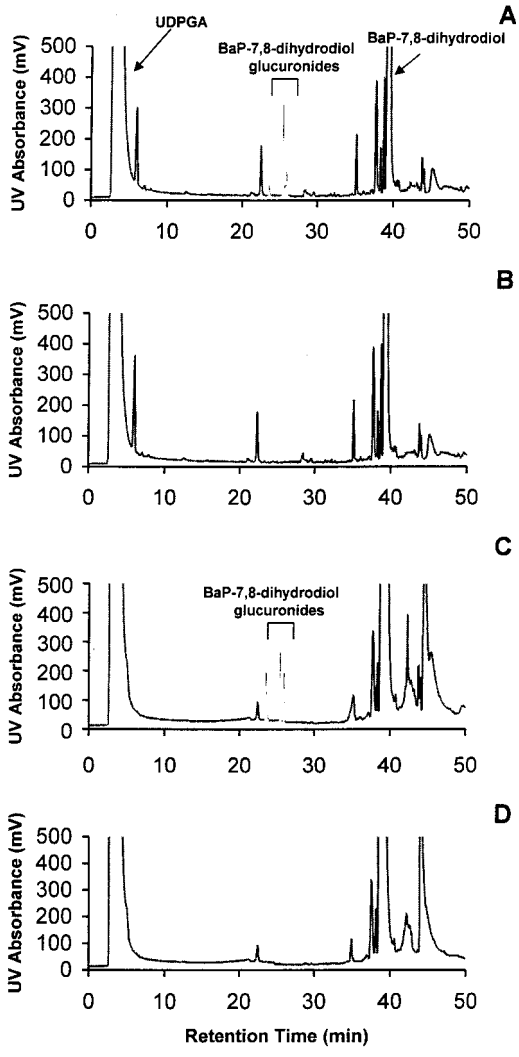

Fig. 5. HPLC analysis of BPD glucuronide formation by human laryngeal and esophageal microsomes. Shown are the UV traces of HPLC separation of metabolites formed in assays using human microsomes (1 mg of protein) incubated with 2 mM racemic BPD and 4 mM UDPGA as described in "Materials and Methods." *A* and *B*, laryngeal microsomes; *C* and *D*, esophageal microsomes. *B* and *D*, assays including β-glucuronidase as described in "Materials and Methods." BPD glucuronide conjugates are indicated.

which cells and tissues protect against BaP-induced carcinogenicity. The results of this study suggest that UGT1A1, UGT1A7, UGT1A8, UGT1A9, and UGT1A10 all exhibit detectable levels of activity against (−)-BPD *in vitro*. Therefore, these UGTs may play an important role in BaP detoxification in human tissues. Previous investigators have suggested that glucuronidation may be an important determinant of individual susceptibility to tobacco-related cancers. For example, it has been hypothesized that smokers with lower urinary ratios of glucuronidated:unconjugated forms of 4-(methylnitrosamino)-1-(3-pyridyl)-1-butanol, a major metabolite of the tobacco-specific nitrosamine 4-(methylnitrosamino)-1-(3-pyridyl)-1-butanone, may be more susceptible to the carcinogenic effects of 4-(methylnitrosamino)-1-(3-pyridyl)-1-butanone and 4-(methylnitrosamino)-1-(3-pyridyl)-1-butanol because these individuals would be less able to detoxify these agents (47). In recent studies, allelic variants of the UGT1A7 gene encoding functionally deficient UGT1A7 isozymes have been strongly associated with increased risk for orolaryngeal cancer (48). Although it remains unclear whether this association is manifested primarily via detoxification of BaP or some other tobacco carcinogen, these data are consistent with the (−)-BPD-glucuronidating activity observed with UGT1A7 and with the similar BPD glucuronide HPLC profiles observed for overexpressed UGT1A7 and aerodigestive tract tissues in this study. They are also consistent with the fact that UGT1A7 is expressed in aerodigestive tract tissues, including those of the oral cavity, larynx, and esophagus (46). Together, these data support a potentially important tobacco carcinogen- and BaP-detoxifying role for UGT1A7 in aerodigestive tract tissues. Studies examining the potential role of other (−)-BPD-metabolizing UGTs in risk for aerodigestive tract and other cancers are currently under way.

The results of the present study strongly implicate several UGT isozymes in the glucuronidation of the important procarcinogen BPD and support recent evidence that glucuronidation is an important detoxification pathway for BaP in multiple tissues. Therefore, several UGT enzymes may serve as important targets for cancer chemoprevention in the future.

ACKNOWLEDGMENTS

We thank Richard D. Beger for obtaining the NMR spectra and Kim Journault for the preparation of membrane fractions of UGT2B17-overexpressing cells.

REFERENCES

1. Gelboin, H. V. Benzo[*a*]pyrene metabolism, activation and carcinogenesis: role and regulation of mixed-function oxidases and related enzymes. Physiol. Rev., *60:* 1107–1166, 1980.
2. IARC Monographs on the Evaluation of the Carcinogenic Risk of Chemicals to Humans. Polynuclear Aromatic Compounds. Part, 1: Chemical, Environmental, and Experimental Data, General Remarks, *32:* 33–91, 1983.
3. Dipple, A., Cheng, S. C., and Bigger, C. A. Polycyclic aromatic hydrocarbon carcinogens. Prog. Clin. Biol. Res., *347:* 109–127, 1990.
4. Borgen, A., Davey, H., Castagnoli, N., Crocker, T. T., Rasmussen, R. E., and Wang, I. Y. Metabolic conversion of benzo[*a*]pyrene by Syrian hamster liver microsomes and binding of metabolites to deoxyribonucleic acid. J. Mol. Chem., *16:* 502–506, 1973.
5. Huberman, E., Sachs, L., Yang, S. K., and Gelboin, H. V. Identification of mutagenic metabolites of benzo[*a*]pyrene in mammalian cells. Proc. Natl. Acad. Sci., *73:* 607–611, 1976.
6. Newbold, R. F., and Brookes, P. Exceptional mutagenicityof a benzo[*a*]pyrene diol epoxide in cultured mammalian cells. Nature (Lond.), *261:* 52–54, 1976.
7. Slaga, T. J., Biaje, A., Berry, D. L., and Bracken, W. M. Identification of mutagenic metabolites of benzo[*a*]pyrene 4,5-, 7,8-, and 7,8-diol-9,10-epoxide and 7,8-diol. Cancer Lett., *2:* 115–122, 1976.
8. Yang, S. K., McCourt, D. W., Leutz, J. C., and Gelboin, H. V. Benzo[*a*]pyrene diol-epoxides. I. Mechanisms of enzymatic formation and optical active intermediates. Science (Wash. DC), *196:* 1199–1201, 1977.
9. Thakker, D. R., Yagi, H., Akagi, H., Koreeda, M., Lu, A. H., Levin, W., Wood, A. W., Conney, A. H., and Jerina, D. Metabolism of benzo[*a*]pyrene VI. Stereoselective metabolism of benzo[*a*]pyrene and benzo[*a*]pyrene 7,8-diol to diol epoxides. Chem. Biol. Interact., *16:* 281–300, 1977.
10. Levin, W., Wood, A. W., Chang, R. L., Ryan, D., Thomas, P. E., Yagi, H., Thakker, D. R., Vyas, K., Boyd, C., Chu, S-Y., Conney, A. H., and Jerina, D. M. Oxidative metabolism of polycyclic aromatic hydrocarbons to ultimate carcinogens. Drug Metab. Rev., *13:* 555–580, 1982.
11. Deutsch, J., Leutz, J., Yang, S. K., Gelboin, H. V., Chiang, Y. L., Vatsis, K. P., and Coon, M. J. Regio- and steroselectivity of various forms of purified cytochrome P-450 in the metabolism of benzo[*a*]pyrene and (−)-trans-7,8-dihydroxy-7,8-dihydrobenzo[*a*]pyrene as shown by product formation and binding to DNA. Proc. Natl. Acad. Sci., *75:* 3123–3127, 1978.
12. Deutsch, J., Vatsis, K., Coon, M. J., Leutz, J., and Gelboin, H. V. Catalytic activity and stereoselectivity of purified forms of rabbit liver microsomal cytochrome P-450 on the oxygenation of the (−) and (+) enantiomers of *trans*-7,8-dihydrobenzo-[*a*]pyrene. Mol. Pharmacol., *16:* 1011–1018, 1979.
13. Tephly, T. R., and Burchell, B. UDP-glucuronosyltransferases: a family of detoxifying enzymes. Trends Pharmacol. Sci., *11:* 276–279, 1990.
14. Gueraud, F., and Paris, A. Glucuronidation: a dual control. Gen. Pharmacol., *31:* 683–688, 1998.
15. Nowell, S. A., Massengill, J. S., Williams, S., Radominska-Pandya, A., Tephly, T. R., Cheng, Z. P., Strassburg, C. P., Tukey, R. H., Macleod, S. L., Lang, N. P., and Kadlubar, F. F. Glucuronidation of 2-hydroxyamino-1-methy-6-phenylimidazo[4,5-*b*]pyridine by human microsomal UDP-glucuronosyltransferases: identification of specific UGT1A family isoforms involved. Carcinogenesis (Lond.), *6:* 1108–1114, 1999.
16. Ren, Q., Murphy, S. E., Zheng, Z., and Lazarus, P. *O*-Glucuronidation of the lung carcinogen 4-(methylnitrosamino)-1-(3- pyridyl)-1-butanol (NNAL) by human UDP-glucuronosyltransferases 2B7 and 1A9. Drug Metab. Dispos., *28:* 1352–1360, 2000.

17. Owens, I. S., and Ritter, J. K. Gene structure at the human UGT1 locus creates diversity in isozyme structure, substrate specificity, and regulation. Prog. Nucleic Acid Res. Mol. Biol., *51:* 305–338, 1995.
18. Jin, C. J., Miners, J. O., Lillywhite, K. J., and Mackenzie, P. I. cDNA cloning and expression of two new members of the human liver UDP-glucuronosyltransferase 2B subfamily. Biochem. Biophys. Res. Commun., *194:* 496–503, 1993.
19. Beaulieu, M., Levesque, E., Tchernof, A., Beatty, B. G., Belanger, A., and Hum, D. W. Chromosomal localization, structure, and regulation of the UGT2B17 gene, encoding a C19 steroid metabolizing enzyme. DNA Cell Biol., *16:* 1143–1154, 1997.
20. Beaulieu, M., Lévesque, É., Hum, D. W., and Bélanger, A. Isolation and characterization of a human orphan UDP-glucuronosyltransferase, UGT2B11. Biochem. Biophys. Res. Commun., *248:* 44–50, 1998.
21. Bélanger, A., Hum, D. W., Beaulieu, M., Lévesque, E., Guillemette, C., Tchernof, A., Bélanger, G., Turgeon, D., and Dubois, S. Characterization and regulation of UDP-glucuronosyltransferases in steroid target tissues. J. Steroid Biochem. Mol. Biol., *65:* 301–310, 1998.
22. Carrier, J. S., Turgeon, D., Journault, K., Hum, D. W., and Bélanger, A. Isolation and characterization of the human UGT2B7 gene. Biochem. Biophys. Res. Commun., *272:* 616–621, 2000.
23. Owens, I., Koteen, G. M., and Legraverend, C. Mutagenesis of certain benzo-[*a*]pyrene phenols *in vitro* following further metabolism by mouse liver. Biochem. Pharmacol., *28:* 1615–1622, 1979.
24. Nemoto, N., Takyama, S., Nagao, M., and Umezawa, K. Modification of the mutagenicity of benzo[*a*]pyrene on bacteria by substrates of enzymes producing water soluble conjugates. Toxicol. Lett., *2:* 205–210, 1978.
25. Hu, Z., and Wells, P. G. *In vitro* and *in vivo* biotransformation and covalent binding of benzo(*a*)pyrene in Gunn and RHA rats with a genetic deficiency in bilirubin uridine diphosphate-glucuronosyltransferase. J. Pharmacol. Exp. Ther., *263:* 334–342, 1992.
26. Hu, Z., and Wells, P. G. Modulation of benzo[*a*]pyrene bioactivation by glucuronidation in lymphocytes and hepatic microsomes from rats with a hereditary deficiency in bilirubin UDP-glucuronosyltransferase. Toxicol. Appl. Pharmacol., *127:* 306–313, 1994.
27. Vienneau, D. S., DeBoni, U., and Wells, P. G. Potential genoprotective role for UDP-glucuronosyltransferases in chemical carcinogenesis: initiation of micronuclei by benzo(*a*)pyrene and benzo(*e*)pyrene in UDP-glucuronosyltransferase-deficient cultured rat skin fibroblasts. Cancer Res., *55:* 1045–1051, 1995.
28. Jin, C. J., Miners, J. O., Burchell, B., and Mackenzie, P. I. The glucuronidation of hydroxylated metabolites of benzo[*a*]pyrene and 2-acetylaminofluorene by cDNA-expressed human UDP-glucuronosyltransferases. Carcinogenesis (Lond.), *14:* 2637–2639, 1993.
29. Grove, A. D., Kessler, F. K., Metz, R. P., and Ritter, J. K. Identification of a rat oltipraz-inducible UDP-glucuronosyltransferase (UGT1A7) with activity towards benzo(*a*)pyrene-7,8-dihydrodiol. J. Biol. Chem., *272:* 1621–1627, 1997.
30. Mojarrabi, B., and Mackenzie, P. I. Characterization of two UDP glucuronosyltransferases that are predominantly expressed in human colon. Biochem. Biophys. Res. Commun., *247:* 704–709, 1998.
31. Strassburg, C. P., Strassburg, A., Nguyen, N., Li, Q., Manns, M. P., and Tukey, R. H. Regulation and function of family 1 and family 2 UDP-glucuronosyltransferase genes (*UGT1A, UGT2B*) in human oesophagus. Biochem. J., *338:* 489–498, 1999.
32. Guillemette, C., Ritter, J. K., Auyeung, D. J., Kessler, F. K., and Housman, D. E. Structural heterogeneity at the UDP-glucuronosyltransferase 1 locus: functional consequences of three novel missense mutations in the human *UGT1A7* gene. Pharmacogenetics, *10:* 629–644, 2000.
33. MacKenzie, P. I., Rodbourn, L., and Iyanagi, T. Glucuronidation of carcinogen metabolites by complementary DNA-expressed uridine 5′-diphosphate glucuronosyltransferases. Cancer Res., *53:* 1529–1533, 1993.
34. Coughtrie, M. W., Burchell, B., and Bend, J. R. Purification and properties of rat kidney UDP-glucuronosyltransferase. Biochem. Pharmacol., *36:* 245–251, 1987.
35. Pritchard, M., Fournel-Gigleux, S., Siest, G., MacKenzie, P., and Magdalou, J. A recombinant phenobarbitol-inducible rat liver UDP-glucuronosyltransferase (UDP-glucuronosyltransferase 2B1) stably expressed in V79 cells catalyzes the glucuronidation of morphine, phenols, and carboxylic acids. Mol. Pharmacol., *45:* 42–50, 1994.
36. Coffman, B. L., Green, M. D., King, C. D., and Tephly, T. R. Cloning and stable expression of a cDNA encoding a rat liver UDP-glucuronosyltransferase (UDP-glucuronosyltransferase 1.1) that catalyzes the glucuronidation of opioids and bilirubin. Mol. Pharmacol., *47:* 1101–1105, 1995.
37. Coffman, B. L., King, C. D., Rios, G. R., and Tephly, T. R. The glucuronidation of opioids, other xenobiotics, and androgens by human UGT2B7Y (268) and UGT2B7H (268). Drug Metab. Dispos., *26:* 73–77, 1998.
38. Green, M. D., Oturo, E. M., and Tephly, T. R. Stable expression of a human liver UDP-glucuronosyltransferase (UGT2B15) with activity toward steroid and xenobiotic substrates. Drug Metab. Dispos., *22:* 799–805, 1994.
39. King, C. D., Rios, G. R., Green, M. D., MacKenzie, P. I., and Tephly, T. R. Comparison of stably expressed rat UGT1.1 and UGT2B1 in the glucuronidation of opioid compounds. Drug Metab. Dispos., *25:* 251–255, 1997.
40. Cheng, Z., Radominska-Pandya, A., and Tephly, T. R. Cloning and expression of human UDP-glucuronosyltransferase (UGT) 1A8. Arch. Biochem. Biophys., *356:* 301–305, 1998.
41. Ebner, T., and Burchell, B. Substrate specificities of two stably expressed human liver UDP-glucuronosyltransferases of the UGT1 gene family. Drug Metab. Dispos., *21:* 50–55, 1993.
42. Ren, Q., Murphy, S. E., Dannenberg, A. J., Park, J. Y., Tephly, T. R., and Lazarus, P. Glucuronidation of the lung carcinogen 4-(methylnitrosamino)-1-(3-pyridyl)-1-butanol (NNAL) by rat UDP-glucuronosyltransferase 2B1. Drug Metab. Dispos., *27:* 1010–1016, 1999.
43. Strassburg, C. P., Manns, M. P., and Tukey, R. H. Expression of the UDP-glucuronosyltransferase 1A locus in human colon. Identification and characterization of the novel extrahepatic UGT1A8. J. Biol. Chem., *273:* 8719–8726, 1998.
44. Strassburg, C. P., Nguyen, N., Manns, M. P., and Tukey, R. H. Polymorphic expression of the UDP-glucuronosyltransferase UGT1A gene locus in human gastric epithelium. Mol. Pharmacol., *54:* 647–654, 1998b.
45. Strassburg, C. P., Kneip, S., Topp, J., Obermayer-Straub, P., Barut, A., Tukey, R. H., and Manns, M. P. Polymorphic gene regulation and interindividual variation of UDP-glucuronosyltransferase activity in human small intestine. J. Biol. Chem., *275:* 36164–36171, 2000.
46. Zheng, Z., Fang, J-L., and Lazarus, P. Glucuronidation: an important mechanism for detoxification of benzo(*a*)pyrene metabolites in aerodigestive tract tissues. Drug Metab. Dispos., in press, 2002.
47. Richie, J. P., Jr., Carmella, S. G., Muscat, J. E., Scott, D. G., Akerkar, S. A., and Hecht, S. S. Differences in the urinary metabolites of the tobacco-specific lung carcinogen 4-(methylnitrosamino)-1-(3-pyridyl)-1-butanone (NNK) in black and white smokers. Cancer Epidemiol. Biomark. Prev., *6:* 783–790, 1997.
48. Zheng, Z. Guillemette, C., Park, J. Y., Schantz, S., and Lazarus, P. The tobacco carcinogen-metabolizing UGT1A7 enzyme: expression in aerodigestive tract tissues and importance of UGT1A7 alleles in risk for oral cancer. J. Natl. Cancer Inst. (Bethesda), *93:* 39–46, 2001.